Bioorganic Chemistry 104 (2020) 104273

Contents lists available at ScienceDirect

Bioorganic Chemistry

journal homepage: www.elsevier.com/locate/bioorg

Synthesis and biological evaluation of β-ionone oriented proapoptosis agents by enhancing the ROS generation

Jie Yang*, Wen-Wen Mu, Yu-Xin Cao, Guo-Yun Liu*

School of Pharmacy, Liaocheng University, 1 Hunan Street, Liaocheng, Shandong 252000, China

ARTICLE INFO

Keywords:
Ionone
Curcumin analog
Reactive oxygen species
Apoptosis

ABSTRACT

β-ionone, a cyclic terpenoid compound present in many fruits, has been showed a broad spectrum of biological activities. In this paper, we synthesized a panel of β-ionone derivatives and tested their anti-proliferation activity on cancer cell by the MTT assay. The results showed that most of the β-ionone derivatives were more active than β-ionone and curcumin. Particularly, the β-ionone derivatives (**1a**, **1d** and **1g**) with *ortho*-substituents on the aromatic ring exhibited much stronger cytotoxicity than their corresponding *meta*- and *para*-substituted compounds. Importantly, the cytotoxicity of the β-ionone derivatives (**1a**, **1d** and **1g**) were relationship with their reactive oxygen species (ROS)-generation abilities, which could lead to the redox imbalance, lipid peroxidation, the loss of mitochondrial membrane potential (MMP), the activation of Bax and Caspase 3, followed by cell apoptosis. This work suggest that the "*ortho effect*", the ROS-generation ability and drawing fluorine atom into drugs may play a potent role in enhancing the anticancer activity of β-ionone derivatives.

1. Introduction

The electrophilic natural products, characterized with Michael acceptor units, have attracted much attention in medicinal chemistry, particularly, in the field of cancer chemoprevention and chemotherapy [1]. The Michael acceptor untis of the electrophilic natrual products could be attacked by the nuclephilic centers of proteins, DNA and glutathione, resulting in a covalent compound with a wide variety of biological functions [2]. α,β-unsaturated ketones, widespread existed in curcumin, β-ionone, chalcone and cinnamic acid derivatives, were a typical Michael acceptor and could remarkebaly enhance the pharmacological properties [3]. Curcumin, as one of the simplest phenolic compound found in turmeric, contains two α,β-unsaturated ketones units and has been used for the purpose of cancer prevention and treatment [4]. In the last few decades, extensive efforts have been devoted to seek new curcumin analogs for the sake of enhancing its stability. Mon-carbonyl curcumin, the representative curcumin analogs, showed more stability and potent anticancer activity *in vitro* than curcumin [5,6].

β-ionone, a cyclic terpenoid compound present in many fruits, vegetables and grains, has been showed a broad spectrum of physiological and pharmacological activities, including anti-inflammatory [7], anticancer [8], antibacterial [9] and tryosine kinase inhibitor [10]. Of particular interest is the anticancer activity of β-ionone, which could induce apoptosis in cancer cell through p53-dependent mitochondrial signaling pathway [11]. Inspired by the anticancer property of monocarbonyl curcumins and β-ionone, a series of β-ionone oriented monocarbonyl curcumin were synthesized by Aldol condension (Scheme 1). Thus, we focus on the structure-activity relationships of these compounds underlying cytotoxic potential on tumor cell lines and probe into the anticancer mechanism against A549 cells.

2. Results and discussion

2.1. Synthesis

The synthetic routs of β-ionone derivatives **1a-m** are depicted in Scheme 1. The desired compounds were synthesized by aldol condensation reaction between β-ionone and respective benzaldehyde in the presence of 20% NaOH aqueous using ethanol as solvent. The title compounds were obtained with medium yields after purification by column chromatography. All compounds were characterized by ^{1}H NMR, ^{13}C NMR and HRMS.

2.2. Cytotoxicity and SAR

All the title compounds were initially tested the cytotoxicity against lung cancer A549 and ovarian cancer SK-OV3 cells, and the results were

* Corresponding author.
E-mail addresses: yangjie1110@163.com (J. Yang), guoyunliu@126.com (G.-Y. Liu).

https://doi.org/10.1016/j.bioorg.2020.104273
Received 28 April 2020; Received in revised form 3 September 2020; Accepted 7 September 2020
Available online 11 September 2020

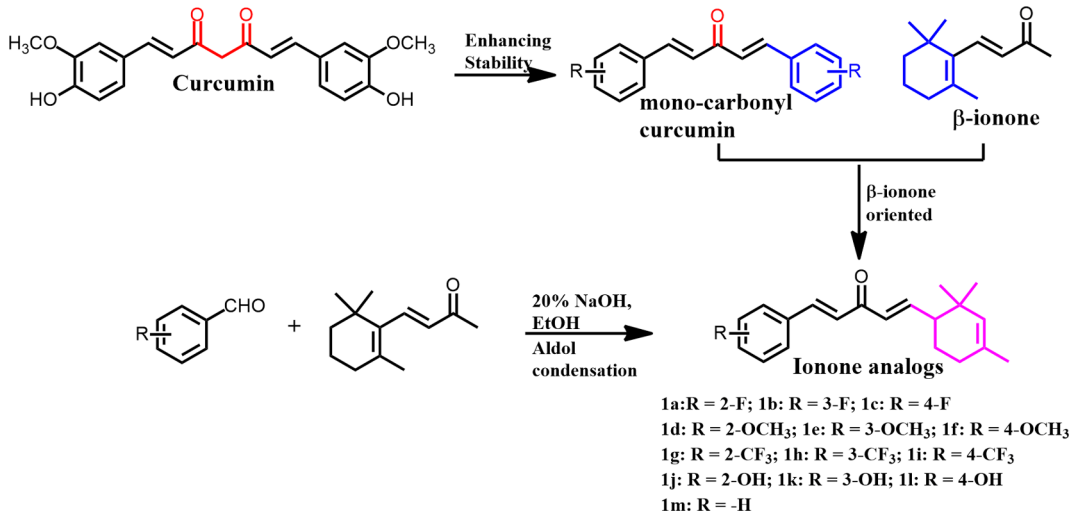

Scheme 1. Molecular structures and synthetic routs of ionone-oriented analogs.

Table 1
Cytotoxicity of β-ionone and its analogs against SK-OV3 and A549 cells.

Comps.	IC_{50} (μM)		Comps.	IC_{50} (μM)	
	SK-OV3	A549		SK-OV3	A549
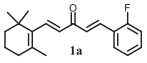	23.4 ± 1.4	19.3 ± 0.6	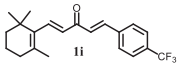	57.8 ± 2.2	40.9 ± 3.6
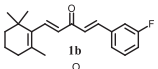	48.9 ± 1.1	19.9 ± 1.4	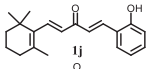	26.0 ± 1.6	37.8 ± 2.7
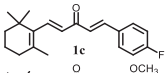	40.6 ± 2.5	18.8 ± 1.2	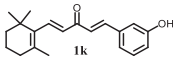	89.4 ± 6.9	39.6 ± 3.4
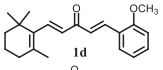	24.2 ± 1.7	37.5 ± 1.4	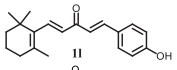	56.8 ± 1.9	60.9 ± 4.7
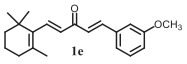	34.0 ± 1.2	36.5 ± 2.3	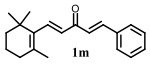	47.6 ± 3.2	32.2 ± 0.7
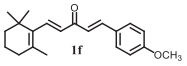	42.2 ± 1.8	65.5 ± 1.1	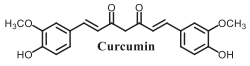	58.1 ± 2.5	53.2 ± 1.1
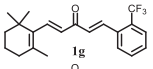	49.9 ± 4.0	20.6 ± 0.4		> 200	> 200
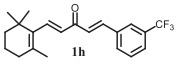	79.6 ± 6.2	46.3 ± 1.8			

[a]The IC_{50} value is the concentration of a compound tested to cause 50% inhibition of cell viability after 48 h of treatment, and is expressed as the mean ± SD for three determinations.

summarized in Table 1. The compounds with substitution at *ortho*- of the aromatic ring exhibited higher cytotoxicity than the corresponding *meta*- and *para*-substituted compounds in SK-OV3 cells. The results were in accordance with the "*ortho* effect" [12], which had been reported in our previous report and could enhance the cytotoxicity of mono-carbonyl curcumin analogs [5]. The "ortho effect" in the cases of A549 cells showed some effect, but not very obvious. The compound **1g** and **1j** (with trifluoromethyl or hydroxyl at *ortho* position) showed much stronger cytotoxicity than the corresponding *meta*- and *para*-trifluoromethyl (**1h** and **1i**) or hydroxyl (**1k** and **1l**) compounds. The "ortho effect" of fluorine or methoxyl substituted compounds showed no abvious in the case of A549 cells. This reason may be relationship with the overexpression of thioredoxin (Trx) and thioredoxin reductase (TrxR) in cancer cells [13,14]. The thioredoxin system, comprising Trx, TrxR and NADPH, is a potent thiol redox system and critical for cell survival and growth [15]. Additionally, drugs, containing Michael acceptor, can irreversibly inhibit the TrxR, and the modified enzyme could trigger ROS generation and then lead cancer cell apoptosis [12]. Therefore, "ortho effect" showed no obvious in the cases of A549 may be due to the overexpression of Trx and TrxR of A549 cells was not consistent with that of SK-OV3 cells.

Compounds, containing Michael acceptor, could trigger ROS generation and then lead cancer cell apoptosis through irreversibly inhibiting the TrxR [12]. Therefore, we subjected β-ionone analogs (**1a**, **1b**, **1c** and **1d**) to TrxR1 (PDBID 2J3N) in docking. As shown in Fig. 1A, the Michael acceptor group of all the four β-ionone analogs were close to the C-terminal Cys498 and the distance was about 3 Å. This suggest that the β-ionone analogs have the potential to interact with the C-terminal Cys-SH of mammalian TrxR. In the other hand, *ortho*-fluorine atom of **1a** may be formed a hydrophobicity interaction with the methyl of Leu409, and *ortho*-methoxyl of **1d** may be formed hydrophilic interaction with the hydroxyl of Trp407. These interactions may be contribute to the inhibition of TrxR by **1a** and **1d** and enhancing the cytotoxicity of compounds with *ortho*-substituents. Further, the molecules with F or CF_3 substituent on the aromatic ring exerted more potent cytotoxicity than that with OH or OMe substituent. This result may

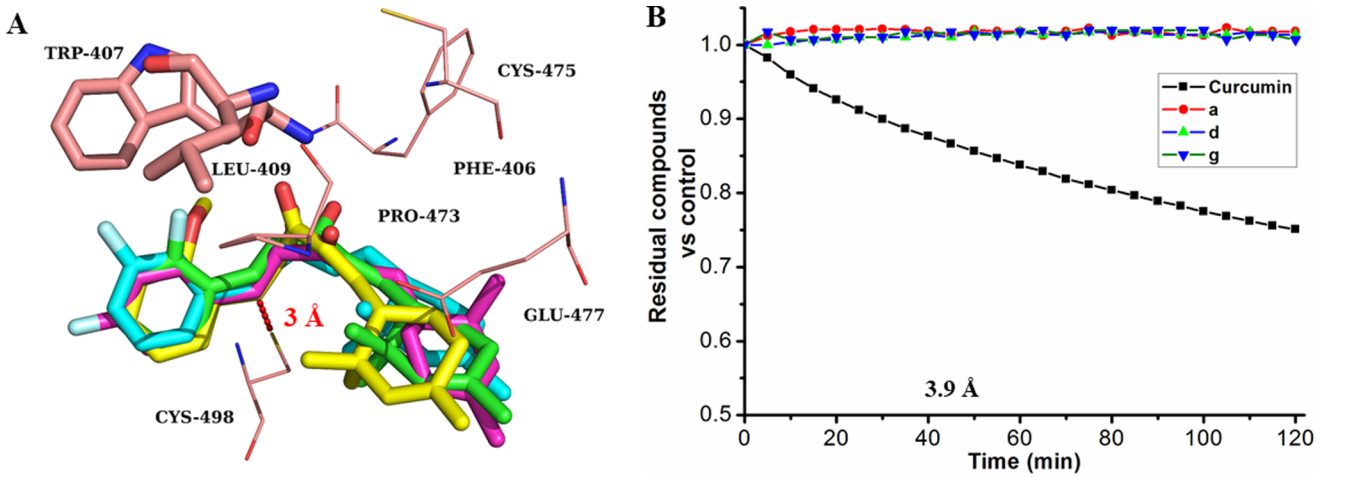

Fig. 1. (A) β-ionone analogs (**1a**, **1b**, **1c** and **1d**) in the binding site of human TrxR1. (B) Stability assessment on curcumin (50 μM) and β-ionone analogs (**1a** (50 μM), **1d** (50 μM) and **1g** (50 μM)) in RPMI 1640 supplemented with 10% (v/v) heat-inactivated fetal calf serum at 25 ˚C by monitoring the decrease in their maximum absorbance.

be due to the fluorine atom, which could increase the lipophilicity and biological activity of the drugs [16]. It is obvious from the results that most of the β-ionone derivatives were more active than that of the leading curcumin and β-ionone. This result was consistent with the more stability of the compounds (**1a**, **1d** and **1g**) than curcumin in RPMI 1640 supplemented with 10% (v/v) heat-inactivated fetal calf serum (Fig. 1**B**). We also found that most of the β-ionone derivatives showed stronger anti-proliferation activity on A549 cells than that on SK-OV3 cells. Therefore, compounds **1a**, **1d** and **1g** were selected for further exploration of the anti-cancer mechanisms against A549 cells.

2.3. β-ionone derivatives induced-ROS generation in A549 cells

ROS, which have been linked to numerous biological processes and disease conditions, is a potent mediator of cytotoxicity [17]. Therefore, we detected the ROS generation induced by β-ionone derivatives (**1a**, **1d** and **1g**) and curcumin in A549 cells with 2′,7′-dichlorofluorescein diacetate (DCFH-DA). As shown in Fig. 2, **1a, 1d and 1g** promoted an extensive increase in the ROS levels in a dose-dependent manner. Especially, β-ionone derivatives (**1a**, **1d** and **1g**) markedly induced much higher ROS production than curcumin. Notablely, compound **1a**, having the strongest anti-proliferation activity against A549 cells, exhibited the most potent ROS-generating ability and induced about 5-fold increase in ROS levels at 60 μM as compared to untreated control cells. These results were in accordance with the cytotoxicity and stability of curcumin and β-ionone derivatives.

2.4. The redox imbalance induced by β-ionone derivatives in A549 cells

An accumulation of ROS, as powerful signaling molecules involved in the regulation of biological processes [17], usually resulted in the redox imbalance, which could be evaluated by the ratio of GSH/GSSG. As our expectation, we started to test whether β-ionone derivatives could result in the redox imbalance of A549 cells. As shown in Fig. 3, we found that the three of β-ionone derivatives (**1a**, **1d** and **1g**) sharply decreased the ratio of GSH/GSSG in a dose-dependent fashion. More important, **1a** exhibited the most severe redox imbalance in A549 cells. In particular, A549 cells treated with 60 μM **1a** displayed about 4-fold decrease in the ratio of GSH/GSSG compared to the control. The activity sequence of **1a**, **1d** and **1g** was in line with their ROS-generating ability. These results also indicated that the sustained flux of ROS frequently brought out redox imbalance.

2.5. The lipid peroxidation induced by β-ionone derivatives in A549 cells

Plasma membrane, playing a critical role in cellular signaling transduction, can be vulnerably attacked by the ROS and resulting in lipid peroxidation [18]. Furthermore, the amount of malondialdehyde

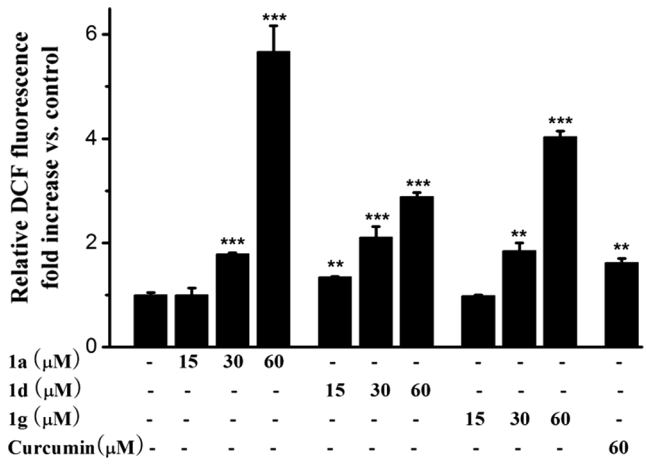

Fig. 2. The ROS generation induced by**1a**, **1d** and **1g** at the indicated concentrations against A549 cells. Each experiment was performed in triplicate.

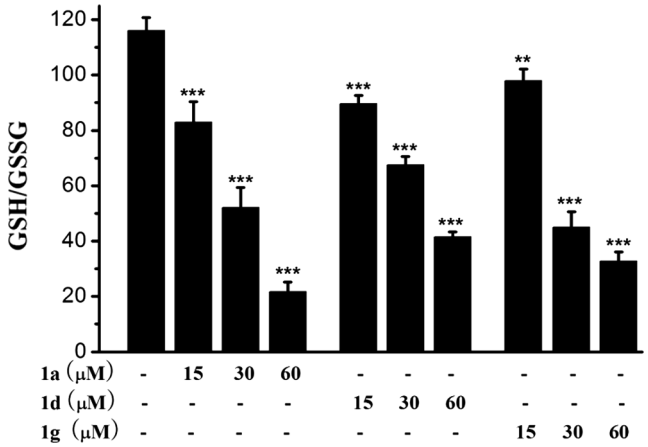

Fig. 3. The changes of GSH/GSSG ratios in A549 cells after treatment with **1a**, **1d and 1g** at the indicated concentrations for 6 h. Each experiment was performed in triplicate.

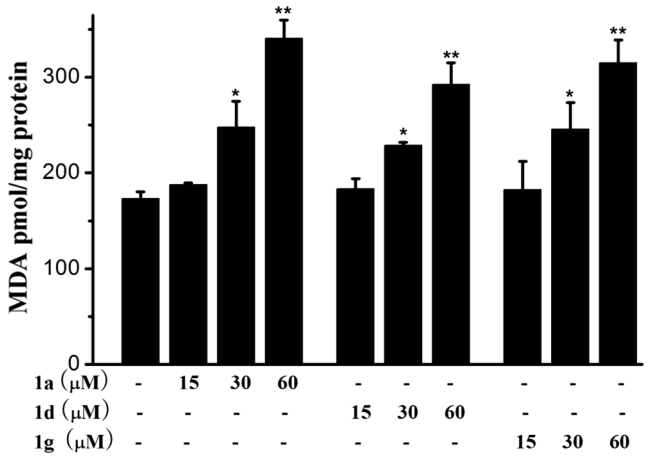

Fig. 4. MDA concentrations of A549 cells was determined after treatment with **1a**, **1d and 1g** at the indicated concentrations for 15 h. Values are expressed as MDA equivalents (pmol)/ mg protein. Each experiment was performed in triplicate.

(MDA), the biomarker of lipid peroxidation, was measured by using thiobarbituric acid-reactive substance. As illustrated in Fig. 4, the formation of MDA was dramatic increase in a dose-dependent manner after treatment with **1a**, **1d** and **1g** at the indicated concentrations. Particularly, 60 μM **1a** caused a 1-fold increase of the amount of MDA compared to the control in A549 cells.

2.6. The loss of mitochondrial membrane potential (MMP) induced by β-ionone derivatives in A549 cells

Mitochondrial, playing a potent role in the regulation of cell survival, can be damaged by the excess ROS [19]. We next determined the loss of mitochondrial membrane potential using rhodamine 123 by flow cytometry. As shown in Fig. 5, we found that the three of the β-ionone derivatives were more active than 60 μM curcumin, and lead to a remarkable decrease in the loss of MMP in a dose-dependent fashion. Especially, 60 μM **1a** brought about an 80% reduction of MMP in A549 cells relative to the control. The abilities of the three β-ionone derivatives (**1a**, **1d** and **1g**) and curcumin were in accordance with their anti-proliferation activities.

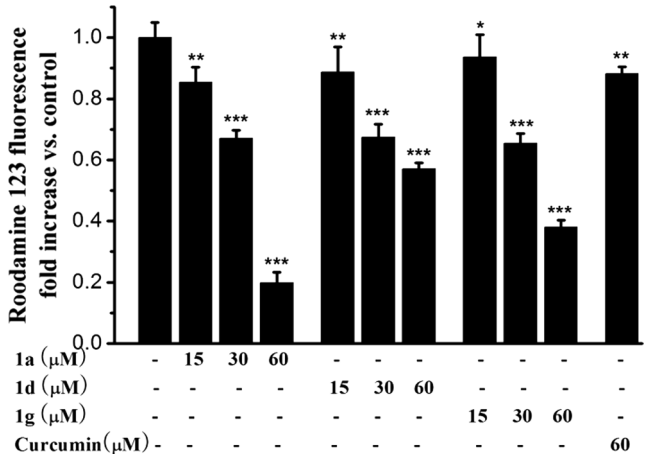

Fig. 5. The loss of mitochondrial membrane potential induced by **1a**, **1d and 1g** at the indicated concentrations in A549 cells for 12 h. Each experiment was performed in triplicate.

2.7. The apoptosis-inducting activity of β-ionone derivatives in A549 cells

Given that the disruption of MMP is a catastrophic event during in apoptosis. Therefore, we determined the effects of β-ionone derivatives (**1a**, **1d** and **1g**) on cells apoptosis by flow cytometry. As illustrated in Fig. 6, the three of β-ionone derivatives were more potent inducer of apoptosis than the leading curcumin, and exhibited perfect dose-dependent manner. Specially, treatment with 60 μM **1a** for 24 h resulted in 51.8% late apoptotic cells. These results suggest that the apoptosis as well the cytotoxicity, the loss of MMP, lipid peroxidation and redox imbalance were in relation with the ROS production triggered by β-ionone derivatives (**1a**, **1d** and **1g)** in A549 cells.

2.8. β-ionone derivatives activated Bax and Caspase 3 expression in A549 cells

Next, we test the proteins expression of Bax and Caspase 3, the well-known apoptosis-regulating proteins, which exhibited a major role in the apoptosis of cancer cells [20]. As a result, compounds **1a** and **1g** could significantly increase the expression level of Bax and Caspase 3 compared with the control group in A549 cells (Fig. 7). Particularly, the expression level of Bax and Caspase 3 proteins promoted by **1g** was more than that of **1a** and **1d**. This result suggested that the β-ionone derivatives-induced apoptosis was mediated through the activation of Bax and Caspase 3.

3. Conclusions

In summary, we synthesized a panel of β-ionone derivatives through Aldol condensation and evaluated their cytotoxicity against A549 and SK-OV3 cells. The results illustrated that **1a**, **1d** and **1g**, with *ortho*-substituents on the aromatic ring, showed much stronger anti-proliferation activity than other β-ionone derivatives. Mechanism investigation hinted that the cytotoxity of β-ionone derivatives were originated from their ROS-generation abilities, which subsequently resulted in the redox imbalance, lipid peroxidation, the collapse of the MMP, the activation of apoptosis-regulating proteins (Bax and Caspase 3) and untimately caused cell apoptosis (Scheme 2). This work revealed that the "*ortho effect*", promoting ROS-generation and the introduction of fluorine atom into drugs may be potent strategies to improve anticancer activity of β-ionone derivatives.

4. Materials and methods

4.1. Materials

Roswell Park Memorial Institute (RPMI)-1640 was from Hyclone. 3-(4,5-dimethylthiazol-2-yl)-2,5-diphenyltetrazolium bromide (MTT), rhodamine 123, 2′,7′-dichlorofluorescein diacetate, reduced L-glutathione (GSH), oxidized L-glutathione (GSSG), 2-vinylpyridine (97%) and thiobarbituric acid were purchased from Beyotime. Annexin V-FITC/PI apoptosis detection kit was from BD Biosciences. RIPA buffer, 50*Cooktail proteinase inhibitor, GAPDH, the primary antibodies and HRP-labeled secondary antibodies were obtained from Servicebio. Substituted benzaldehyde, β-ionone and curcumin were from EnergyChemical. All other chemicals were of the highest quality available.

4.2. Synthesis of the β-ionone oriented mono-carbonyl curcumin analogs

*4.2.1. General procedure for the synthesis of **1a-1i***

The mono-carbonyl curcumin analogs were synthesized according to the published procedure [21]. Briefly, the aqueous NaOH (20%, w/v, 6 mL) was added dropwise to the mixture, containing β-ionone (5 mmol) and various subsstituted benzaldehyde (5 mmol) in ethanol (15 mL), at 0 °C. After completion of the reaction, distilled water

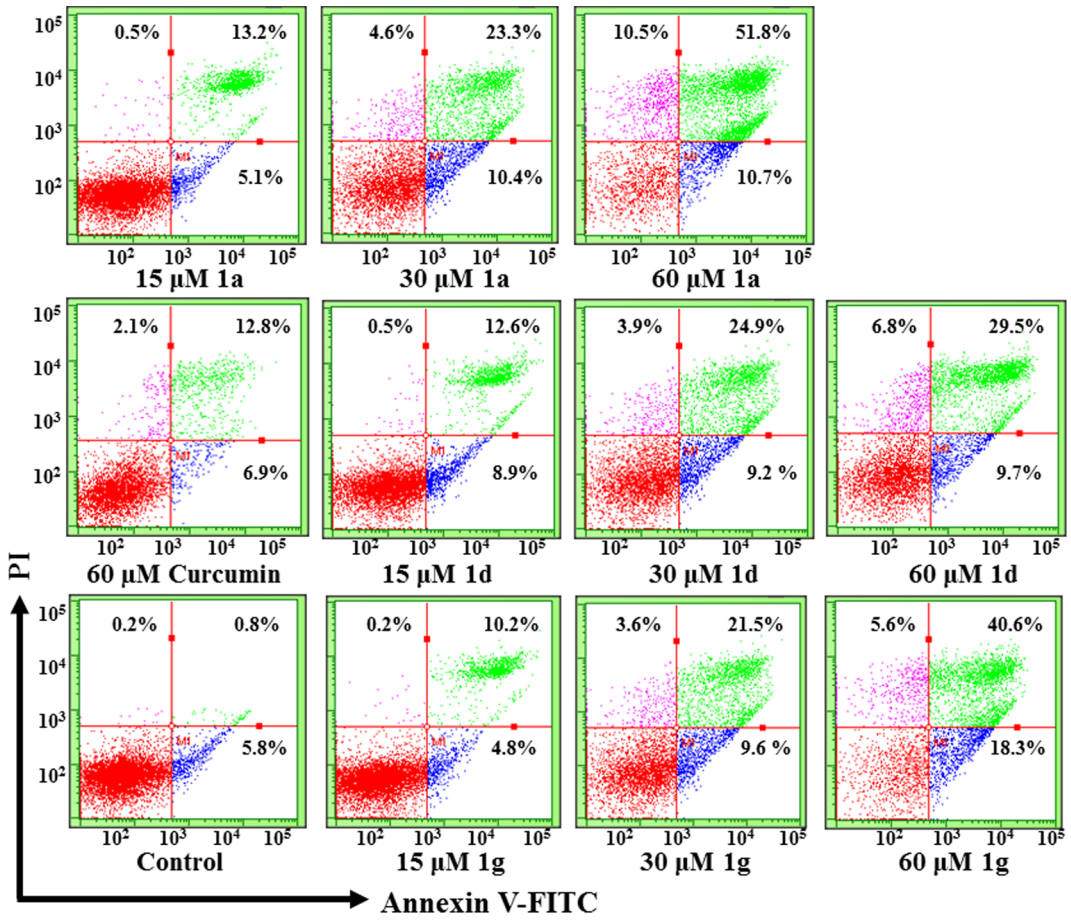

Fig. 6. Flow cytometric analysis for apoptotic induction of A549 cells treated with curcumin and β-ionone derivatives (**1a**, **1d** and **1g**) for 24 h. Each experiment was performed in triplicate.

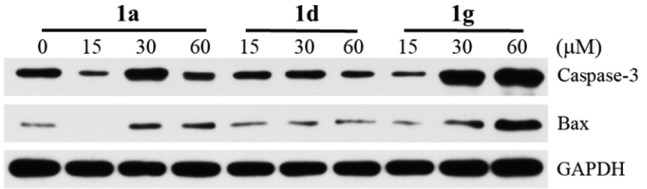

Fig. 7. Effects of β-ionone derivatives (**1a**, **1d** and **1g**) on the activation of Bax and Caspase 3 in A549 cells for 18 h.

(20 mL) was addeed, the mixture was neutralized with 10% hydrochloric acid solution and extracted with EtOAc. Then, the organic solvent was removed and the residue was purified by a silica gel column. Their structures were confirmed by ^{1}H, ^{13}C NMR and HRMS spectroscopy.

(1*E*,4*E*)-1-(2-fluorine-phenyl)-5-(2,6,6-trimethylcyclohex-1-en-1-yl) penta-1,4-dien-3-one (1a) : Yield 31.7%, yellow solid, ^{1}H NMR (400 MHz, ($CDCl_3$), δ 7.76 (d, J = 16.0 Hz, 1H), 7.58 (t, J = 8.0 Hz, 1H), 7.50 (d, J = 16.0 Hz, 1H), 7.33–7.39 (m, 1H), 7.16 (t, J = 8.0 Hz, 1H), 7.09 (t, J = 8.0 Hz, 1H), 7.07 (d, J = 16.0 Hz, 1H), 6.47 (d, J = 16.0 Hz, 1H), 2.09 (t, J = 8.0 Hz, 2H), 1.83 (s, 3H), 1.61–1.66 (m, 2H), 1.49–1.52 (m, 2H), 1.12 (s, 6H); ^{13}C NMR (100 MHz, $CDCl_3$), δ 189.3, 162.8, 160.3, 143.5, 137.0, 136.5, 135.3, 135.2, 131.7, 131.6, 129.4, 129.3, 128.0, 124.5, 124.4, 116.3, 116.1, 39.8, 34.2, 33.7, 28.9, 21.9, 18.9. HRMS *m/z* (ES^+): $[M+H]^+$ 299.1821 (theor 299.1811).

(1*E*,4*E*)-1-(3-fluorine-phenyl)-5-(2,6,6-trimethylcyclohex-1-en-1-yl) penta-1,4-dien-3-one (1b): Yield 36.4%, yellow solid, ^{1}H NMR (400 MHz, ($CDCl_3$), δ 7.59 (d, J = 16.0 Hz, 1H), 7.50 (d, J = 16.0 Hz, 1H), 7.35–7.38 (m, 2H), 7.27 (d, J = 8.0 Hz, 1H), 7.08–7.10 (m, 1H), 6.96 (d, J = 16.0 Hz, 1H), 6.44 (d, J = 16.0 Hz, 1H), 2.09 (t, J = 8.0 Hz, 2H), 1.83 (s, 3H), 1.62-–1.65 (m, 2H), 1.49–1.52 (m, 2H), 1.12 (s, 6H); ^{13}C NMR (100 MHz, $CDCl_3$), δ 188.8, 164.2, 161.8, 143.5, 141.2, 141.1, 137.3, 137.2, 136.5, 130.5, 130.4, 129.4, 126.7, 124.4, 124.3, 117.2, 117.0, 114.4, 114.2, 39.8, 34.2, 33.7, 28.9, 21.9, 18.9. HRMS *m/z* (ES^+): $[M+H]^+$ 299.1825 (theor 299.1811).

(1*E*,4*E*)-1-(4-fluorine-phenyl)-5-(2,6,6-trimethylcyclohex-1-en-1-yl) penta-1,4-dien-3-one (1c): Yield 40.8%, yellow solid, ^{1}H NMR (400 MHz, ($CDCl_3$), δ 7.61 (d, J = 16.0 Hz, 1H), 7.56 (dd, J = 8.0 Hz, 2H), 7.49 (d, J = 16.0 Hz, 1H), 7.07 (t, J = 8.0 Hz, 2H), 6.90 (d, J = 16.0 Hz, 1H), 6.44 (d, J = 16.0 Hz, 1H), 2.09 (t, J = 8.0 Hz, 2H), 1.83 (s, 3H), 1.63–1.66 (m, 2H), 1.49–1.52 (m, 2H), 1.11 (s, 6H); ^{13}C NMR (100 MHz, $CDCl_3$), δ 189.0, 165.1, 162.6, 143.3, 141.4, 137.0, 136.5, 130.2, 130.1, 129.4, 125.3, 116.2, 115.9, 39.8, 34.2, 33.7, 28.9, 21.9, 18.9. HRMS *m/z* (ES^+): $[M+H]^+$ 299.1826 (theor 299.1811).

(1*E*,4*E*)-1-(2-methoxy-phenyl)-5-(2,6,6-trimethylcyclohex-1-en-1-yl)penta-1,4-dien-3-one (1d): Yield 35.2%, yellow oil, ^{1}H NMR (400 MHz, ($CDCl_3$), δ 7.98 (d, J = 16.0 Hz, 1H), 7.58 (d, J = 8.0 Hz, 1H), 7.46 (d, J = 16.0 Hz, 1H), 7.34 (t, J = 8.0 Hz, 1H), 7.05 (d, J = 16.0 Hz, 1H), 6.96 (t, J = 8.0 Hz, 1H), 6.92 (d, J = 8.0 Hz, 1H), 6.48 (d, J = 16.0 Hz, 1H), 3.90 (s, 3H), 2.08 (t, J = 8.0 Hz, 2H), 1.82 (s, 3H), 1.63–1.66 (m, 2H), 1.49–1.52 (m, 2H), 1.11 (s, 6H); ^{13}C NMR (100 MHz, $CDCl_3$), δ 189.9, 158.5, 142.8, 138.2, 136.6, 136.0, 131.5, 129.7, 128.8, 126.4, 123.9, 120.7, 111.1, 55.5, 39.8, 34.2, 33.6, 28.9, 21.9, 18.9. HRMS *m/z* (ES^+): $[M+H]^+$ 311.2025 (theor 311.2011).

(1*E*,4*E*)-1-(3-methoxy-phenyl)-5-(2,6,6-trimethylcyclohex-1-en-1-yl)penta-1,4-dien-3-one (1e): Yield 32.4%, yellow solid, ^{1}H NMR (400 MHz, ($CDCl_3$), δ 7.61 (d, J = 16.0 Hz, 1H), 7.49 (d, J = 16.0 Hz, 1H), 7.30 (t, J = 8.0 Hz, 1H), 7.18 (d, J = 8.0 Hz, 1H),7.11 (s, 1H),

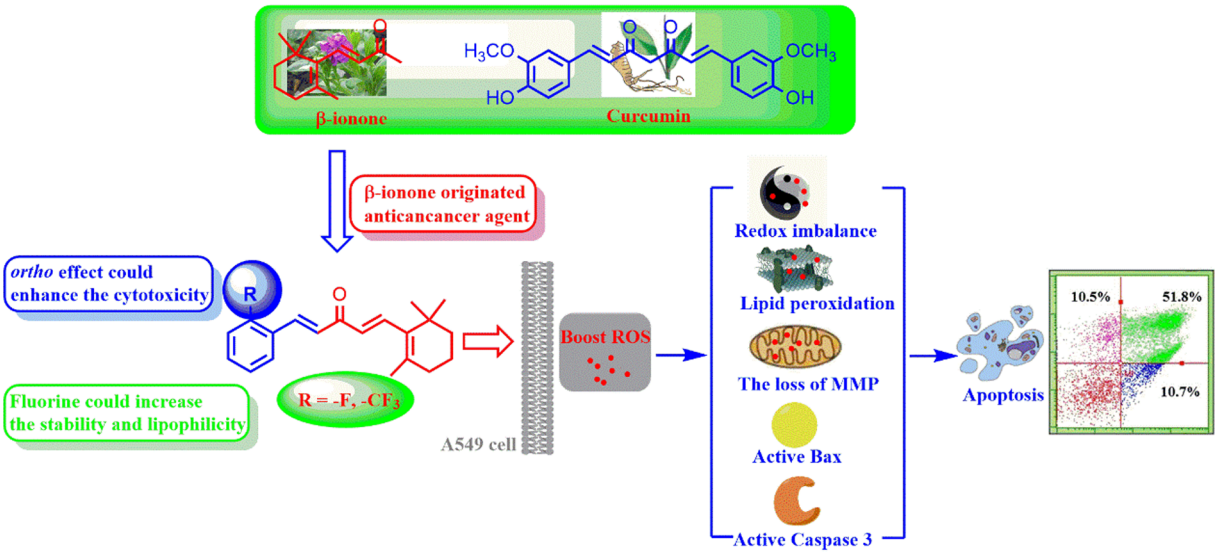

Scheme 2. β-ionone derivatives induce A549 apoptosis via enhancing ROS generation.

6.96 (d, J = 16.0 Hz, 1H), 6.93 (t, J = 8.0 Hz, 1H), 6.46 (d, J = 16.0 Hz, 1H), 3.85 (s, 3H), 2.09 (t, J = 8.0 Hz, 2H), 1.83 (s, 3H), 1.61–1.64 (m, 2H), 1.49–1.52 (m, 2H), 1.11 (s, 6H); ^{13}C NMR (100 MHz, $CDCl_3$), δ 189.1, 159.9, 143.2, 142.6, 136.8, 136.5, 136.3, 129.9, 129.4, 126.0, 121.0, 116.1, 113.1, 55.3, 39.8, 34.2, 33.7, 28.9, 21.9, 18.9. HRMS m/z (ES^+): $[M+H]^+$ 311.2024 (theor 311.2011).

(1*E*,4*E*)-1-(4-methoxy-phenyl)-5-(2,6,6-trimethylcyclohex-1-en-1-yl)penta-1,4-dien-3-one (1f): Yield 40.5%, yellow oil, ^{1}H NMR (400 MHz, ($CDCl_3$), δ 7.62 (d, J = 16.0 Hz, 1H), 7.54 (d, J = 8.0 Hz, 2H), 7.46 (d, J = 16.0 Hz, 1H), 6.91 (d, J = 8.0 Hz, 2H), 6.86 (d, J = 16.0 Hz, 1H), 6.44 (d, J = 16.0 Hz, 1H), 3.85 (s, 3H), 2.08 (t, J = 8.0 Hz, 2H), 1.82 (s, 3H), 1.63–1.66 (m, 2H), 1.49–1.51 (m, 2H), 1.11 (s, 6H); ^{13}C NMR (100 MHz, $CDCl_3$), δ 189.1, 161.4, 142.6, 142.5, 136.6, 136.2, 130.0, 129.7, 127.6, 123.6, 114.4, 55.4, 39.8, 34.2, 33.7, 28.9, 21.9, 18.9. HRMS m/z (ES^+): $[M+H]^+$ 311.2026 (theor 311.2011).

(1*E*,4*E*)-1-(2-trifluoromethy-phenyl)-5-(2,6,6-trimethylcyclohex-1-en-1-yl)penta-1,4-dien-3-one (1 g): Yield 38.7%, yellow oil, ^{1}H NMR (400 MHz, ($CDCl_3$), δ 7.98 (d, J = 16.0 Hz, 1H), 7.77 (d, J = 8.0 Hz, 1H), 7.71 (d, J = 8.0 Hz, 1H), 7.57 (t, J = 8.0 Hz, 1H), 7.50 (d, J = 16.0 Hz, 1H), 7.47 (t, J = 8.0 Hz, 1H), 6.89 (d, J = 16.0 Hz, 1H), 6.50 (d, J = 16.0 Hz, 1H), 2.09 (t, J = 8.0 Hz, 2H), 1.84 (s, 3H), 1.61–1.66 (m, 2H), 1.49–1.52 (m, 2H), 1.12 (s, 6H); ^{13}C NMR (100 MHz, $CDCl_3$), δ 189.1, 143.8, 138.0, 137.4, 136.5, 132.1, 130.2, 130.0, 129.7, 129.5, 128.6, 127.8, 126.2, 39.8, 34.2, 33.8, 28.8, 21.8, 18.9. HRMS m/z (ES^+): $[M+H]^+$ 349.1808 (theor 349.1779).

(1*E*,4*E*)-1-(3-trifluoromethy-phenyl)-5-(2,6,6-trimethylcyclohex-1-en-1-yl)penta-1,4-dien-3-one (1 h): Yield 39.7%, yellow solid, ^{1}H NMR (400 MHz, ($CDCl_3$), δ 7.83 (s, 1H), 7.74 (d, J = 8.0 Hz, 1H), 7.65 (d, J = 16.0 Hz, 1H), 7.63 (d, J = 8.0 Hz, 1H), 7.53 (t, J = 8.0 Hz, 1H), 7.51 (d, J = 8.0 Hz, 1H), 7.03 (d, J = 16.0 Hz, 1H), 6.47 (d, J = 16.0 Hz, 1H), 2.10 (t, J = 8.0 Hz, 2H), 1.84 (s, 3H), 1.61–1.66 (m, 2H), 1.50–1.52 (m, 2H), 1.13 (s, 6H); ^{13}C NMR (100 MHz, $CDCl_3$), δ 188.6, 143.7, 140.6, 137.4, 136.5, 135.8, 131.3, 129.4, 129.2, 127.3, 126.6, 126.5, 124.6, 39.9, 34.2, 33.8, 28.9, 21.9, 18.9. HRMS m/z (ES^+): $[M+H]^+$ 349.1801 (theor 349.1779).

(1*E*,4*E*)-1-(4-trifluoromethy-phenyl)-5-(2,6,6-trimethylcyclohex-1-en-1-yl)penta-1,4-dien-3-one (1i): Yield 42.6%, yellow solid, ^{1}H NMR (400 MHz, ($CDCl_3$), δ 7.68 (d, J = 8.0 Hz, 1H), 7.66 (d, J = 16.0 Hz, 2H), 7.64 (d, J = 8.0 Hz, 2H), 7.52 (d, J = 16.0 Hz, 1H), 7.04 (d, J = 16.0 Hz, 1H), 6.46 (d, J = 16.0 Hz, 1H), 2.10 (t, J = 8.0 Hz, 2H), 1.84 (s, 3H), 1.62–1.66 (m, 2H), 1.50–1.52 (m, 2H), 1.12 (s, 6H); ^{13}C NMR (100 MHz, $CDCl_3$), δ 188.7, 143.8, 140.6, 138.4, 137.5, 136.5, 129.3, 128.3, 127.7, 125.9, 125.8, 39.8, 34.2, 33.8, 28.9, 21.9, 18.9. HRMS m/z (ES^+): $[M+H]^+$ 349.1807 (theor 349.1779).

(1*E*,4*E*)-1-(2-hydroxy-phenyl)-5-(2,6,6-trimethylcyclohex-1-en-1-yl) penta-1,4-dien-3-one (1j): Yield 26.3%, yellow solid, ^{1}H NMR (400 MHz, ($CDCl_3$), δ 8.07 (d, J = 16.0 Hz, 1H), 7.75 (s, 1H), 7.55 (d, J = 16.0 Hz, 1H), 7.53 (d, J = 8.0 Hz, 1H), 7.24 (t, J = 8.0 Hz, 1H), 7.22 (d, J = 16.0 Hz, 1H), 6.95 (d, J = 8.0 Hz, 1H), 6.90 (t, J = 8.0 Hz, 1H), 6.54 (d, J = 16.0 Hz, 1H), 6.38 (s, 1H), 2.09 (t, J = 8.0 Hz, 2H), 1.84 (s, 3H), 1.63–1.65 (m, 2H), 1.49–1.52 (m, 2H), 1.12 (s, 6H); ^{13}C NMR (100 MHz, $CDCl_3$), δ 191.1, 156.3, 143.6, 139.8, 137.2, 129.1, 126.1, 122.1, 120.4, 116.8, 39.8, 34.2, 33.8, 28.9, 21.9, 18.9. HRMS m/z (ES^+): $[M+H]^+$ 297.1869 (theor 297.1855).

(1*E*,4*E*)-1-(3-hydroxy-phenyl)-5-(2,6,6-trimethylcyclohex-1-en-1-yl) penta-1,4-dien-3-one (1 k): Yield 28.8%, yellow oil, ^{1}H NMR (400 MHz, ($CDCl_3$), δ 7.62 (d, J = 16.0 Hz, 1H), 7.53 (d, J = 16.0 Hz, 1H), 7.25 (t, J = 8.0 Hz, 1H), 7.14 (d, J = 8.0 Hz, 1H), 7.14 (s, 1H), 6.97 (d, J = 16.0 Hz, 1H),6.91 (d, J = 16.0 Hz, 1H), 6.47 (d, J = 16.0 Hz, 1H), 6.38 (s, 1H), 2.09 (t, J = 8.0 Hz, 2H), 1.83 (s, 3H), 1.62–1.65 (m, 2H), 1.48–1.51 (m, 2H), 1.11 (s, 6H); ^{13}C NMR (100 MHz, $CDCl_3$), δ 189.9, 156.6, 143.9, 143.3, 137.8, 136.5, 136.2, 130.1, 129.1, 125.7, 120.6, 117.9, 115.1, 39.8, 34.2, 33.8, 28.9, 21.9, 18.9. HRMS m/z (ES^+): $[M+H]^+$ 297.1870 (theor 297.1855).

(1*E*,4*E*)-1-(4-hydroxy-phenyl)-5-(2,6,6-trimethylcyclohex-1-en-1-yl) penta-1,4-dien-3-one (1 l): Yield 30.5%, yellow oil, ^{1}H NMR (400 MHz, ($CDCl_3$), δ 7.65 (d, J = 16.0 Hz, 1H), 7.53 (d, J = 16.0 Hz, 1H), 7.53 (s, 1H), 7.47 (d, J = 8.0 Hz, 2H), 6.86 (d, J = 16.0 Hz, 1H),6.49 (d, J = 16.0 Hz, 1H), 2.08 (t, J = 8.0 Hz, 2H), 1.82 (s, 3H), 1.62–1.65 (m, 2H), 1.48–1.51 (m, 2H), 1.11 (s, 6H); ^{13}C NMR (100 MHz, $CDCl_3$), δ 190.3, 159.1, 144.0, 143.6, 137.6, 136.5, 130.5, 129.2, 126.8, 122.9, 116.2, 39.8, 34.2, 33.8, 28.9, 21.9, 18.9. HRMS m/z (ES^+): $[M+H]^+$ 297.1867 (theor 297.1855).

(1*E*,4*E*)-1-phenyl-5-(2,6,6-trimethylcyclohex-1-en-1-yl)penta-1,4-dien-3-one (1 m): Yield 26.9%, yellow solid, ^{1}H NMR (400 MHz, ($CDCl_3$), δ 7.65 (d, J = 16.0 Hz, 1H), 7.58 (dd, J = 8.0, 4.0 Hz, 2H), 7.49 (d, J = 16.0 Hz, 1H), 7.39–7.40 (m, 3H), 6.98 (d, J = 16.0 Hz, 1H), 6.46 (d, J = 16.0 Hz, 1H), 2.09 (t, J = 8.0 Hz, 2H), 1.83 (s, 3H), 1.63–1.64 (m, 2H), 1.49–1.52 (m, 2H), 1.12 (s, 6H); ^{13}C NMR (100 MHz, $CDCl_3$), δ 189.2, 143.2, 142.8, 136.8, 136.5, 134.9, 130.3, 129.5, 128.9, 128.3, 125.6, 39.8, 34.2, 33.7, 28.9, 21.9, 18.9. HRMS m/z (ES^+): $[M+H]^+$ 281.1921 (theor 281.1905).

4.3. MTT assay

Human lung cancer cells (A549) and human ovarian cancer cells (SK-OV3), which were from the Shanghai Institute of Biochemistry and Cell Biology, Chinese Academy of Sciences, were grown and maintained in RPMI-1640 medium at 37 ˚C in a humidified atmosphere with 5% CO_2. A549 (3×10^3/well) and SK-OV3 cells (5×10^3/well) were plated in 96-well plates, then incubated with vehicle alone or the tested compounds at the indicated concentrations for 48 h. Subsequently, the MTT assay was done to evaluate the cytotoxic potential as reported previously [22,23].

4.4. Stability assay

The stability of curcumin and ionone-oriented analogs, dissolving in RPMI 1640 supplemented with 10% (v/v) heat-inactivated fetal calf serum, was monitored at their maximun absorbance for 120 min at 10-min intervals as described previously [24].

4.5. Cell apoptosis analysis

A549 (3×10^5) cells were incubated in 6-well plates and treated with vehicle alone or the tested compounds at the indicated concentrations for 24 h. The cells were harvested, washed with PBS and labeled with FITC Annexin-V and PI as described previously [24]. Subsequently, the samples were analyzed by using a flow cytometry.

4.6. Intracellular ROS measurement

A549 (3×10^5) cells were seeded in 6-well plates and incubated with the vehicle alone or the tested compounds at the indicated concentrations for 6 h. The cells were collected, washed with PBS and stained with DCFH-DA at the dark. Then, the cells were washed with PBS and resuspended in PBS followed by analyzing with a flow cytometry.

4.7. Measurement of GSH and GSSG levels

A549 (3×10^5 cells/well) cells were cultured in 6-well plates and incubated for 24 h. After treatment with the tested compounds at the indicated concentrations for 6 h, the cells were harvested, washed with PBS and lysed. Then, the intracellular GSH and GSSG content were determined by the glutathione reductase-DTNB recycling [25].

4.8. Determination of thiobarbituric acid-reactive substance (TBARS)

A549 cells were cultured at 3×10^5 cells/well in 6-well plates and incubated for 24 h. After incubation with the vehicle alone or the test compounds for 18 h, the cells were harvested and lysed. Then, the samples were tested by the protocol as previously described [26].

4.9. Analysis of mitochondrial membrane potential

A549 cells were plated at 3×10^5 cells/well in 6-well plates and incubated for 24 h. The cells were incubated with the vehicle alone or the test compounds for 18 h. Then, the cells were harvested, washed with PBS and stained with Rhodamine 123 for 30 min at 37 ˚C. After washing with PBS, the samples were analyzed using a flow cytometry as previously reported [24].

4.10. Western blotting analysis

The expression of Bax and Caspase 3 proteins after treatment with the test compounds were analyzed by western blot as previously descripted [27]. In brief, A549 cells were seeded at a density of 3×10^5 cells/well in 6-well plates and treated with the test compounds for 18 h. Cells were collected, washed three times with ice-cold phosphate-buffered saline and lysed with ice-cold RIPA lysis buffer containing proteinase inhibitors. Then, the equal amounts of protein were separated on SDS-PAGE and blotted onto PVDF membranes. The membranes were blocked with 5% skim milk and probed with the primary antibodies before incubation with the corresponding HRP-labeled secondary antibody. After washing, the blotted protein were detected with enhanced chemiluminescence (ECL).

4.11. Molecular docking simulation

Crystal structure of human TrxR1 was downloaded from RCSB PDB database (http://www.rcsb.org) with PDBID 2J3N. The protein was prepared according to AutoDock 4.2 manual: The bound ligand was extracted from the complexes, water molecules were removed, and hydrogen and charge were automatically added. The ligands were energy minimized with MM2 force field using ChemBioOffice 2014 (http://www.cambridgesoft.com), and the prepared structures were used as input files for docking. The grid box of 60 Å size (x, y, z) with a spacing of 0.375 Å was created representing the active binding site where contained the native ligand and all the important amino acids. Finally, the best pose of Figure was showed by pyMol [28].

4.12. Statistical analysis

The data was expressed as the mean ± SD of at least three independent experiments. Significant differences ($P < 0.05$) between the means of two groups are analyzed by Student's *t*-test.

Declaration of Competing Interest

The authors declare that they have no known competing financial interests or personal relationships that could have appeared to influence the work reported in this paper.

Acknowledgments

This work was supported by the National Natural Science Foundation of China (Grant No. 81901420), Shandong Provincial Natural Science Foundation (Grant No. ZR2018LH022), the Open Project of Shandong Collaborative Innovation Centre for Antibody Drugs (Grant No. CIC-AD1822 and CIC-AD1824).

Appendix A. Supplementary material

Supplementary data to this article can be found online at https://doi.org/10.1016/j.bioorg.2020.104273.

References

[1] M. Gersch, J. Kreuze, S.A. Sieber, Electrophilic natural products and their biological targets, Nat. Prod. Rep. 29 (2012) 659–682.
[2] Y. Nakamura, N. Miyoshi, Electrophiles in foods: the current status of isothiocyanates and their chemical biology, Biosci. Biotechnol. Biochem. 74 (2010) 242–255.
[3] S. Krishnan, R.M. Miller, B.X. Tian, R.D. Mullins, M.P. Jacobson, J. Taunton, Design of reversible, cysteine-targeted Michael acceptors guided by kinetic and computational analysis, J. Am. Chem. Soc. 136 (2014) 12624–12630.
[4] J. Chen, Z.M. He, F.L. Wang, Z.S. Zhang, X.Z. Liu, D.D. Zhai, W.D. Chen, Curcumin and its promise as an anticancer drug: An analysis of its anticancer and antifungal effects in cancer and associated complications from invasive fungal infections, Eur. J. Pharmacol. 772 (2016) 33–42.
[5] G.Y. Liu, Q. Zhai, J.Z. Chen, Z.Q. Zhang, J. Yang, 2,2′-Fluorine mono-carbonyl curcumin induce reactive oxygen species-Mediated apoptosis in Human lung cancer NCI-H460 cells, Eur. J. Pharmacol. 786 (2016) 161–168.
[6] G.Y. Liu, C.C. Jia, P.R. Han, J. Yang, 3,5-Bis(2-fluorobenzylidene)-4-piperidone induce reactive oxygen species-mediated apoptosis in A549 cells, Med. Chem. Res. 27 (2018) 128–136.
[7] Z. NowakowskaZ, A review of anti-infective and anti-inflammatory chalcones, Eur. J. Med. Chem. 42 (2007) 125–137.

[8] P. Singh, R. Raj, V. Kumar, M.P. Mahajan, P.M.S. Bedi, T. Kaur, A.K. Saxena, 1,2,3-Triazole tethered β-lactam-Chalcone bifunctional hybrids: Synthesis and anticancer evaluation, Eur. J. Med. Chem. 47 (2012) 594–600.
[9] V. Sharma, G. Singh, H. Kaur, A.K. Saxena, M.P.S. Ishar, Synthesis of β-ionone derived chalcones as potent antimicrobial agents, Bio. Med. Chem. Lett. 22 (2012) 6343–6346.
[10] O. Nerya, R. Musa, S. Khatib, S. Tamir, J. Vaya, Chalcones as potent tyrosinase inhibitors: the effect of hydroxyl positions and numbers, Phytochemistry 65 (2004) 1389–1395.
[11] J. Zhu, L. Zhang, X.M. Jin, X.Y. Han, C.H. Sun, J.L. Yan, β-Ionone-induced apoptosis in human osteosarcoma (U2os) cells occurs via a p53-dependent signaling pathway, Mol. Biol. Rep. 37 (2010) 2653–2663.
[12] F. Dai, G.Y. Liu, Y. Li, W.J. Yan, Q. Wang, J. Yang, D.L. Lu, D. Lin, B. Zhou, Insights into the importance for designing curcumin-inspired anticancer agents by a prooxidant strategy: The case of diarylpentanoids, Free Radic. Biol. Med. 85 (2015) 127–137.
[13] K. Kahlos, Y. Soini, M. Säily, P. Koistinen, S. Kakko, P. Pääkkö, A. Holmgren, V.L. Kinnula, Up-regulation of thioredoxin and thioredoxin reductase in human malignant pleural mesothelioma, Int. J. Cancer 95 (2001) 198–204.
[14] Y. Soini, K. Kahlos, U. Näpänkangas, R. Kaarteenaho-Wiik, M. Säily, P. Koistinen, P. Pääkkö, A. Holmgren, V.L. Kinnula, Widespread expression of thioredoxin and thioredoxin reductase in non-small cell lung carcinoma, Clin. Cancer Res. 7 (2001) 1750–1757.
[15] E.H. Chew, A.A. Nagle, Y.C. Zhang, S. Scarmagnani, P. Palaniappan, T.D. Bradshaw, A. Holmgren, A.D. Westwell, Cinnamaldehydes inhibit thioredoxin reductase and induce Nrf2: potential candidates for cancer therapy and chemoprevention, Free Radic. Biol. Med. 48 (2010) 98–111.
[16] T. Naret, J. Bignon, G. Bernadat, M. Benchekroun, H. Levaique, C. Lenoir, J. Dubois, A. Pruvost, F. Saller, D. Borgel, B. Manoury, V. Leblais, R. Darrigrand, S. Apcher, J.D. Brion, E. Schmitt, F. Leroux, M. Alami, A. Hamze, A fluorine scan of a tubulin polymerization inhibitor isocombretastatin A-4: Design, synthesis, molecular modelling, and biological evaluation, Eur. J. Med. Chem. 143 (2018) 473–490.
[17] S. Galadari, A. Rahman, S. Pallichankandy, F. Thayyullathil, Reactive oxygen species and cancer paradox: To promote or to suppress? Free Radic. Biol. Med. 104 (2017) 144–164.
[18] J. Trouverie, G. Vidal, Z. Zhang, C. Sirichandra, K. Madiona, Z. Amiar, J.L. Prioul, E. Jeannette, J.P. Rona, M. Brault, Anion channel activation and proton pumping inhibition involved in the plasma membrane depolarization induced by ABA in *Arabidopsis thaliana* suspension cells are both ROS dependent, Plant Cell Physiol. 49 (2008) 1495–1507.
[19] A.B. Kunnumakkara, P. Anand, B.B. Aggarwal, Mobilized $CD34^+$ cells as a biomarker candidate for the efficacy of combined maximal tolerance dose and continuous infusional chemotherapy and G-CSF surge in gastric cancer, Cancer Lett. 269 (2008) 199–225.
[20] A. Boice, L. Bouchier-Hayes, Targeting apoptotic caspases in cancer, BBA-Mol. Cell Res. 1867 (2020) 118688.
[21] V. Sharma, A. Chaudhary, S. Arora, A.K. Saena, M.P.S. Ishar, β-Ionone derived chalcones as potent antiproliferative agents, Eur. J. Med. Chem. 69 (2013) 310–315.
[22] N.H. Metwally, E.A. Deeb, Synthesis, anticancer assessment on human breast, liver and colon carcinoma cell lines and molecular modeling study using novel pyrazolo [4,3-*c*]pyridine derivatives, Bioorg. Chem. 77 (2018) 203–214.
[23] A.H. Abdelazeem, M.T. EI-Saadi, E.G. Said, B.G.M. Youssif, H.A. Omar, S.M. EI-Moghazy, Novel diphenylthiazole derivatives with multi-target mechanism: Synthesis, docking study, anticancer and anti-inflammatory activities. Bioorg. Chem. 75(2017) 127-138.
[24] G.Y. Liu, Y.Z. Sun, N. Zhou, X.M. Du, J. Yang, S.J. Guo, 3,3′-OH curcumin causes apoptosis in HepG2 cells through ROS-mediated pathway, Eur. J. Med. Chem. 112 (2016) 157–163.
[25] C. Vandeputte, T. Guizon, T. Genestie-Denis, B. Vannier, G. Lorenzon, A microtiter plate assay for total glutathione and glutathione disulfide contents in cultured/isolated cells: performance study of a new miniaturized protocol, Cell Biol. Toxicol. 10 (1994) 415–421.
[26] X.Z. Bao, F. Dai, Q. Wang, X.L. Jin, B. Zhou, Developing glutathione-activated catechol-type diphenylpolyenes as small molecule-based and mitochondria-targeted prooxidative anticancer theranostic prodrugs, Free Radic. Biol. Med. 134 (2019) 406–418.
[27] Y.Y. Ma, Z.M. Di, Q. Cao, W.S. Xu, S.X. Bi, J.S. Yu, Y.J. Shen, Y.Q. Yu, Y.X. Shen, L.J. Feng, Xanthatin induces glioma cell apoptosis and inhibits tumor growth via activating endoplasmic reticulum stress-dependent CHOP pathway, Acta Pharmacol. Sin. 41 (2020) 404–414.
[28] J.M. Zhang, Y.P. Liu, D.F. Shi, G.D. Hu, B.X. Zhang, X.M. Li, R.J. Liu, X. Han, X.J. Yao, J.G. Fang, Synthesis of naphthazarin derivatives and identification of novel thioredoxin reductase inhibitor as potential anticancer agent, Eur. J. Med. Chem. 140 (2017) 435–447.